Pressure and temperature effects on intermolecular vibrational dynamics of ionic liquids

Tatiana C. Penna, Luiz F. O. Faria, Jivaldo R. Matos, and Mauro C. C. Ribeiro

Citation: J. Chem. Phys. **138**, 104503 (2013); doi: 10.1063/1.4793760
View online: http://dx.doi.org/10.1063/1.4793760
View Table of Contents: http://jcp.aip.org/resource/1/JCPSA6/v138/i10
Published by the American Institute of Physics.

Pressure and temperature effects on intermolecular vibrational dynamics of ionic liquids

Tatiana C. Penna,[1] Luiz F. O. Faria,[1] Jivaldo R. Matos,[2] and Mauro C. C. Ribeiro[1,a)]
[1]*Laboratório de Espectroscopia Molecular, Instituto de Química, Universidade de São Paulo, CP 26077, CEP 05513-970 São Paulo, SP, Brazil*
[2]*Laboratório de Análises Térmicas Ivo Giolitto, Instituto de Química, Universidade de São Paulo, CP 26077, CEP 05513-970 São Paulo, SP, Brazil*

(Received 24 December 2012; accepted 15 February 2013; published online 11 March 2013)

Low frequency Raman spectra of ionic liquids have been obtained as a function of pressure up to ca. 4.0 GPa at room temperature and as a function of temperature along the supercooled liquid and glassy state at atmospheric pressure. Intermolecular vibrations are observed at ∼20, ∼70, and ∼100 cm^{-1} at room temperature in ionic liquids based on 1-alkyl-3-methylimidazolium cations. The component at ∼100 cm^{-1} is assigned to librational motion of the imidazolium ring because it is absent in non-aromatic ionic liquids. There is a correspondence between the position of intermolecular vibrational modes in the normal liquid state and the spectral features that the Raman spectra exhibit after partial crystallization of samples at low temperatures or high pressures. The pressure-induced frequency shift of the librational mode is larger than the other two components that exhibit similar frequency shifts. The lowest frequency vibration observed in a glassy state corresponds to the boson peak observed in light and neutron scattering spectra of glass-formers. The frequency of the boson peak is not dependent on the length scale of polar/non-polar heterogeneity of ionic liquids, it depends instead on the strength of anion–cation interaction. As long as the boson peak is assigned to a mixing between localized modes and transverse acoustic excitations of high wavevectors, it is proposed that the other component observed in Raman spectra of ionic liquids has a partial character of longitudinal acoustic excitations. © *2013 American Institute of Physics*. [http://dx.doi.org/10.1063/1.4793760]

I. INTRODUCTION

Vibrational dynamics of intermolecular degrees of freedom of glass-forming liquids has been intensively studied in the last years because of several relationships that have been proposed between short time (picoseconds) dynamics and structural relaxation or transport coefficients of viscous liquids. For instance, Larini *et al.*[1] showed a universal scaling of the logarithm of the viscosity or structural relaxation time by the mean squared displacement within a short time regime in which a molecule experiences rattling dynamics inside the cage of neighboring molecules. Dyre[2] reviewed elastic models of supercooled liquids in which the activation energy of viscous flow is assigned to elastic moduli at infinite frequency. A theory relating the activation energy of viscosity to a quantity that, rather than being a constant, is instead temperature dependent, $\ln \eta \propto E_a(T)/kT$, would be able to explain the non-Arrhenius behavior, i.e., the fragility of supercooled liquids. Thus, $E_a(T)$ has been related to the configurational entropy in the Adam-Gibbs theory,[3] the free volume by Turnbull and Cohen,[4] and the above mentioned fast dynamics.[1,2]

Many of the so-called ionic liquids,[5] formerly called room temperature molten salts, are good glass-forming liquids. The melting temperature of an ionic liquid is $T_m < 373$ K by convention and differential scanning calorimetry (DSC) measurements have shown that typical glass transition temperature is $T_g \sim 190$ K.[6–9] The complex molecular structure of typical ionic liquids might suppress ionic packing in a crystalline array so that the viscous liquid is easily supercooled and eventually becomes a glass rather than a crystal. Motivated by both the technological applications and the fundamental scientific issues, a growing literature on structure and dynamics of ionic liquids has become available in the last decade using different spectroscopic techniques.[5,10–18] In the low-frequency range, ionic liquids dynamics have been investigated by optical Kerr effect (OKE),[10–15] far-infrared,[16,17] terahertz time domain,[16,18] dielectric relaxation,[13,14] and Raman spectroscopies.[16] OKE spectroscopy has been the most commonly used technique for unraveling the intermolecular vibrational dynamics of ionic liquids within the THz range.[5] On the other hand, low frequency Raman spectroscopy ($5 < \omega < 100$ cm^{-1}) also provides important insights on the intermolecular dynamics of supercooled ionic liquids as it probes polarizability fluctuation like OKE spectroscopy.[19,20]

In this work, we consider the effect of pressure on low frequency Raman spectra of ionic liquids, in contrast to previous investigations focusing only on the effect of temperature.[19,20] Ionic liquids under high pressure have been studied by Raman spectroscopy in the high frequency range of intramolecular normal modes. These studies showed conformational changes,[21,22] phase transitions,[23–25] and enhancement of anion–cation hydrogen bonding interactions,[26] for several ionic liquids under high pressure. However, in the authors' knowledge, there is no previous study concerning the effect of pressure on the low frequency range of Raman or

a)Author to whom correspondence should be addressed. Electronic mail: mccribei@iq.usp.br.

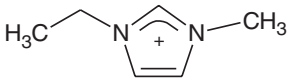

1-ethyl-3-methylimidazolium

$[C_2C_1im]^+$

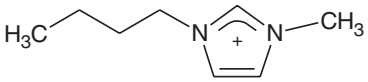

1-butyl-3-methylimidazolium

$[C_4C_1im]^+$

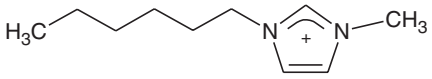

1-hexyl-3-methylimidazolium

$[C_6C_1im]^+$

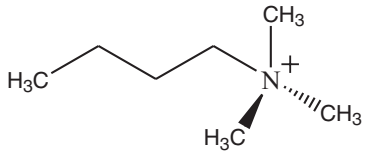

butyltrimethylammonium

$[C_4C_1C_1C_1N]^+$

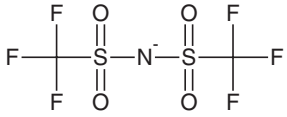

bis(trifluromethanesulfonyl)imide

$[Tf_2N]^-$

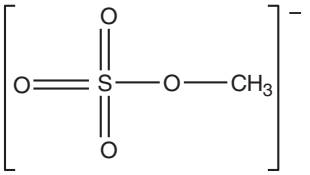

methylsulphate

$[C_1SO_4]^-$

Br^-, bromide

FIG. 1. Ionic structures and notation of the species investigated in this work.

OKE spectra of ionic liquids. In case of molecular and polymeric glass-formers,[27] the evident modifications in the Raman spectrum resulting from applying pressure are the reduction of the quasi-elastic scattering intensity that is related to fast relaxations, and the upward frequency shift of the so-called boson peak, which is a broad band related to intermolecular vibrations within the THz range. Although these high pressure effects on Raman spectra are analogous to low temperature effects, Hong *et al.*[27–29] have shown that a comparison between pressure and temperature variations allows discriminating between the role played by free volume and purely thermal effects on the dynamics of viscous liquids.

The systematic modification of molecular structures of anions and cations has been the main approach to understand the nature of intermolecular vibrations in Raman and OKE spectra of ionic liquids. On the other hand, pressure is an important variable because the effect of pressure is usually much larger than the effect of temperature on the vibrational frequency and Raman band shapes. Interestingly, we observed crystallization under high pressure in an ionic liquid that did not crystallize during cooling in DSC measurements. In contrast, DSC measurements discussed below indicate that an easily crystallized supercooled ionic liquid had crystallization frustrated in a binary mixture with another structurally related system. Thus, by changing temperature and pressure on different ionic liquids, it is the aim of this work to unravel the underlying microscopic origin of the characteristic features of low frequency Raman spectra of ionic liquids.

II. EXPERIMENTAL

The ionic liquids were purchased from Iolitec and used without further purification. The ionic liquids were dried under high vacuum (below 10^{-5} mbar) for at least 48 h before measurements. Figure 1 shows schematic structures and notation of the ionic species used in this work. The systems actually investigated were: $[C_2C_1im][Tf_2N]$, $[C_4C_1im][Tf_2N]$, $[C_6C_1im][Tf_2N]$, $[C_4C_1im][C_1SO_4]$, $[C_6C_1im]Br$, $[C_4C_1C_1C_1N][Tf_2N]$. In order to prevent crystallization of supercooled $[C_2C_1im][Tf_2N]$, binary mixtures of $[C_2C_1im][Tf_2N]$ and $[C_6C_1im][Tf_2N]$ have been done with different molar fractions according to the density of pure components, respectively, 1.5192 and 1.370 g cm^{-3}.[30,31] It will be shown that a molar fraction as low as $x = 0.1$ of $[C_6C_1im][Tf_2N]$ is enough to prevent crystallization while cooling $[C_2C_1im][Tf_2N]$.

Thermophysical characterization of some of these ionic liquids was performed with a differential scanning calorimeter model DTA-50 (Shimadzu) using aluminum pans, hermetically sealed using a sample encapsulating press. Liquid nitrogen was used as a coolant. The sample was first heated above room temperature to remove crystal nuclei eventually present

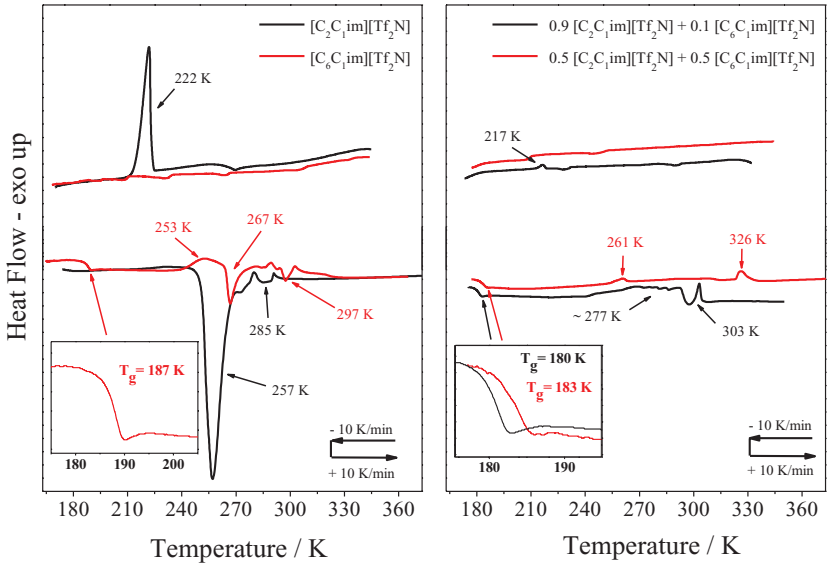

FIG. 2. DSC scans of pure $[C_2C_1im][Tf_2N]$ and $[C_6C_1im][Tf_2N]$ (black and red lines, respectively, in the left panel), and binary mixtures $[C_2C_1im][Tf_2N]$–$[C_6C_1im][Tf_2N]$ with molar fraction $x = 0.1$ and $x = 0.5$ of $[C_6C_1im][Tf_2N]$ (black and red lines, respectively, in the right panel).

in the liquid phase, then it was cooled to ca. 180 K at a rate of 10 K min^{-1}, and it was heated again above room temperature.

Raman spectra as a function of temperature at atmospheric pressure were obtained with a Jobin-Yvon T64000 triple monochromator spectrometer equipped with CCD in the usual 90° scattering geometry with no selection of polarization of the scattered radiation. Temperature control was achieved with an Optistat^{DN} cryostat (Oxford Instruments) and the spectra were excited with the 647.1 nm line of a mixed argon-krypton Coherent laser. Raman spectra as a function of pressure at room temperature were obtained with a Jobin-Yvon T64000 triple monochromator focusing the 632.8 nm line from a He-Ne laser onto the sample by a 20× objective. High pressure was achieved with a diamond anvil cell (DAC) from EasyLab Technologies Ltda, model Diacell® Bragg-XVue, having a diamond culet size of 500 μm. The Boehler microDriller (EasyLab) was used to drill a 250 μm hole in a stainless steel gasket (10 mm diameter, 250 μm thick) preindented to ∼150 μm. Pressure calibration has been done by the usual method of measuring the shift of the fluorescence line of ruby.[32] The spectral resolution was 2.0 cm^{-1} in both the temperature and the pressure dependent measurements.

III. RESULTS

A. Thermal analysis

Attempts to obtain Raman spectra of deeply supercooled liquid and glassy phase of systems containing the $[C_2C_1im]^+$ cation showed that it is not easy to avoid crystallization while supercooling $[C_2C_1im]^+$ based ionic liquids.[9,33] We found that crystallization of $[C_2C_1im][Tf_2N]$ could be avoided in binary mixtures with $[C_6C_1im][Tf_2N]$, even in mixtures containing only a small amount of $[C_6C_1im][Tf_2N]$. This finding is confirmed in Figure 2, which compares DSC scans of pure $[C_2C_1im][Tf_2N]$ and pure $[C_6C_1im][Tf_2N]$ (left panel) and $[C_2C_1im][Tf_2N]$–$[C_6C_1im][Tf_2N]$ binary mixtures (right panel) with molar fractions $x = 0.1$ and 0.5 of the latter.

Freezing and melting temperatures of pure $[C_2C_1im][Tf_2N]$, $T_f = 222$ K and $T_m = 257$ K, agree with previous results of Fredlake *et al.*,[9] although we were not able to identify a signature of glass transition of $[C_2C_1im][Tf_2N]$ at $T_g = 181$ K as in Ref. 9. In line with the thermophysical characterization of $[C_6C_1im][Tf_2N]$ performed by Blokhin *et al.*,[7] we found $T_g = 187$ K for pure $[C_6C_1im][Tf_2N]$ and a complex DSC scan indicating cold crystallization while reheating the system through the supercooled liquid phase. Blokhin *et al.*[7] showed that depending on the thermal conditions, three different crystalline phases of $[C_6C_1im][Tf_2N]$ could be obtained within the $205 < T < 260$ K range followed by melting of these crystals at $T_m = 272$ K. In the single heating scan of $[C_6C_1im][Tf_2N]$ shown in Fig. 2, this complex phase behavior corresponds to the broad exothermic event above T_g and melting at ∼267 K. The right panel of Fig. 2 indicates that crystallization has been suppressed along the cooling scan of $[C_2C_1im][Tf_2N]$–$[C_6C_1im][Tf_2N]$ binary mixtures. Complex events of cold crystallization can be discerned by broad thermal events observed while reheating the binary mixtures. Recently, Annat *et al.*[34] also showed that crystallization could be avoided in binary mixtures of some ionic liquids based on the $[Tf_2N]^-$ anion, for instance, mixtures containing $[C_2C_1im]^+$ and the *N*-methyl-*N*-propylpyrrolidinium cation. In fact, a well-known recipe to avoid crystallization leading to glass formation is to use mixtures, either molecular liquids or molten salts, metallic alloys, or even binary mixtures of Lennard-Jones atomic species in models for computer simulations.[35]

Figure 3 shows DSC scan of $[C_6C_1Im]Br$, for which no crystallization was observed. The cooling DSC trace shows small steps due to noise and the only reproducible thermal event is related to the glass transition observed in the heating trace at $T_g \sim 182$ K. This finding is in line with results of

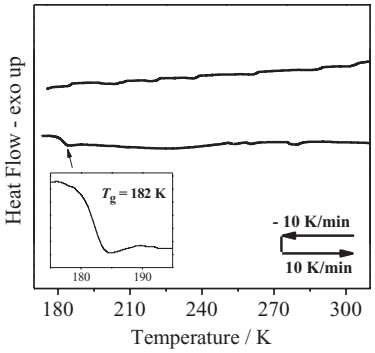

FIG. 3. DSC scan of $[C_6C_1im]Br$.

Imanari *et al.*[36] showing that crystallization of a related system, namely $[C_4C_1Im]Br$, takes place at an extremely slow rate during heating of the sample. On the other hand, an interesting contrast between $[C_6C_1Im][Tf_2N]$ and $[C_6C_1Im]Br$ was found while recording Raman spectra under high pressures: $[C_6C_1Im][Tf_2N]$ does not crystallize for pressures up to 4.3 GPa, whereas $[C_6C_1Im]Br$ crystallizes already at $P \sim 1.4$ GPa. Most probably, the much more complex molecular structure of the $[Tf_2N]^-$ anion with several conformations in comparison with the simple Br^- anion hinders crystallization of $[C_6C_1Im][Tf_2N]$, whereas $[C_6C_1Im]Br$ crystallizes within this pressure range. In fact, in a previous work we showed that partial crystallization of supercooled $[C_4C_1C_1C_1N][Tf_2N]$ could be achieved with the $[Tf_2N]^-$ anion either in *cisoid* or in *transoid* conformation just by changing the cooling rate.[37] The role of high pressures on the interplay between molecular conformations and phase transitions of ionic liquids is yet less understood than the role of the thermal history. Nevertheless, some detailed DSC investigations have been published showing that complex DSC scans of ionic liquids result from slow conformational dynamics.[36,38,39] The analysis of DSC measurements performed by Nishikawa *et al.*[38,39] suggested that conformational changes of 1-alkyl-3-methylimizadolium cations take place as slow cooperative motions that affect local melting and/or crystallization, so that crystalline domains might remain even above the melting temperature.

B. Raman spectra

We showed in previous works that the phenomenology of low frequency Raman spectra of ionic liquids along the supercooled liquid and glassy phases is characteristic of glass-forming liquids:[19,20] there is a strong reduction of the quasi-elastic scattering (QES) intensity at T_g so that the underlying low frequency vibrations are clearly seen at low temperatures. In order to decrease the strong QES intensity centred at zero wavenumber, Raman spectra will be shown here in the usual susceptibility representation[40] $\chi''(\omega) = I(\omega)/[n(\omega)+1]$, where $I(\omega)$ is the raw Raman spectrum and $n(\omega) = [\exp(h\omega/kT)\text{-}1]^{-1}$ is a thermal population factor. An overview of differences between temperature and pressure effects on $\chi''(\omega)$ spectra for a given system is provided in Figure 4 for the ionic liquid $[C_6C_1im][Tf_2N]$. The QES intensity decreases either by decreasing temperature or increasing pressure, but the effect of

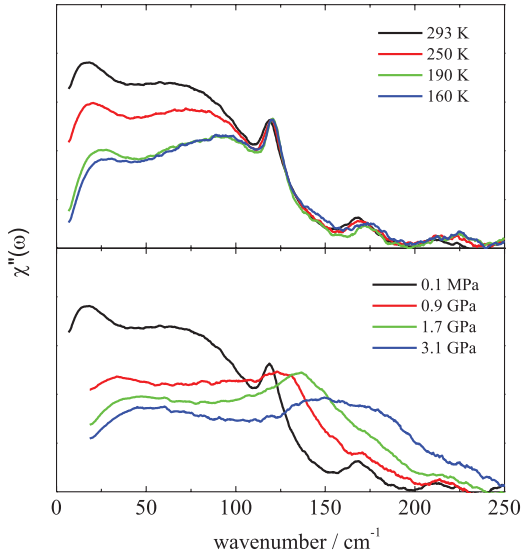

FIG. 4. Raman spectra in the susceptibility representation of $[C_6C_1im][Tf_2N]$ as a function of temperature at atmospheric pressure (top panel) and as a function of pressure at room temperature (bottom panel).

temperature on vibrational frequencies is mild in comparison with the effect of pressure. The sharp band observed at room temperature and atmospheric pressure at $\sim$120 cm^{-1} is assigned to an intramolecular normal mode of $[Tf_2N]^-$ because it is present only in ionic liquids based on this anion. The vibrational frequency of this $[Tf_2N]^-$ normal mode is essentially unchanged at low temperatures, but it experiences significant frequency shift under high pressures. The spectra shown in the top panel of Fig. 4 also indicate the occurrence of an intermolecular vibration at $\sim$100 cm^{-1}, which strongly overlaps with the $[Tf_2N]^-$ normal mode as pressure increases (bottom panel). The pressure effect on frequencies and widths implies an overall broader band shape of $\chi''(\omega)$ spectra at high pressures. Nevertheless, the same procedure used in previous works of curve fit to Raman and OKE spectra of ionic liquids can be also applied here for the pressure dependent spectra.

Details on the procedure of curve fit of low frequency spectra of ionic liquids as a function of temperature has been given in previous publications.[10,12,19,20] Briefly, the QES intensity is usually fit by a lorentzian function centered at zero wavenumber. Being the QES assigned to fast relaxation processes, the other low frequency bands that are observed at non-zero frequencies are assigned to intermolecular vibrational dynamics. A log-normal band is used to fit the component at $\sim$20 cm^{-1} and two gaussian functions for the components at $\sim$70 cm^{-1} and $\sim$100 cm^{-1}. In case of ionic liquids containing $[Tf_2N]^-$, another lorentzian function is needed to fit the characteristic normal mode of this anion at 120 cm^{-1}. We stress that such curve fits are intended to obtain the pressure induced frequency shift of the intermolecular vibrations, rather than a definitive account of the exact band shape of each individual component.

Some examples of such curve fit procedure are shown in Figure 5 for the $\chi''(\omega)$ spectra of $[C_4C_1im][C_1SO_4]$ as a function of pressure. The low frequency Raman spectra in Fig. 5

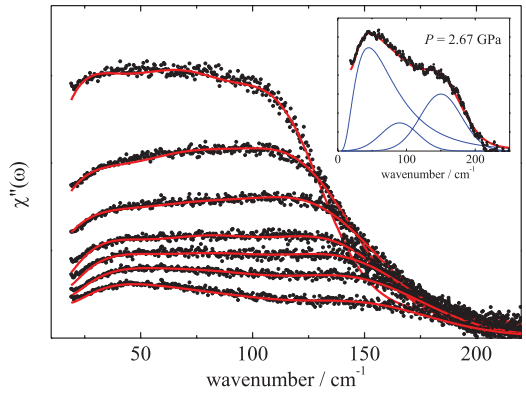

FIG. 5. Raman spectra in the susceptibility representation of $[C_4C_1im][C_1SO_4]$ as a function of pressure (black dots) and corresponding curve fits (red line). From the high to low intensity, the pressures are: 0.24, 0.35, 0.80, 1.04, 1.53, 2.09, and 2.67 GPa. The inset shows the 2.67 GPa data with the intermolecular vibrations of the curve fit shown as blue lines.

are relatively more simple than $[C_6C_1im][Tf_2N]$ (Fig. 4) because there is not the overlapping $[Tf_2N]^-$ band in case of $[C_4C_1im][C_1SO_4]$. On the other hand, there is a considerable simplification of the spectrum for ionic liquids that are not based on aromatic cations because there is not the intermolecular dynamics at $\sim$100 cm^{-1}. This is illustrated in Figure 6 by $\chi''(\omega)$ spectra of $[C_4C_1C_1C_1N][Tf_2N]$, for which it is also clear that vibrational frequencies are essentially unchanged at low temperature in comparison with large frequency shifts under high pressure.

Figure 7 shows the frequency shifts of these bands as a function of pressure for the ionic liquids $[C_4C_1im][C_1SO_4]$ (top panel) and $[C_6C_1im][Tf_2N]$ (bottom panel). The magnitude of the pressure-induced shift of the librational band (circles) is distinct from the other two bands that exhibit similar shifts (squares and triangles in Fig. 7). As long as the Raman band at $\sim$100 cm^{-1} has been assigned to librational motion of the imidazolium ring (see discussion below), the pressure induced shifts shown in Fig. 7 suggest that the underlying dynamics are distinct for the other two bands at lower frequencies.

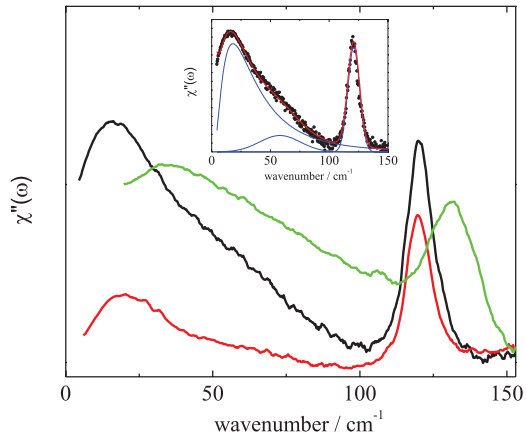

FIG. 6. Pressure and temperature effects on the Raman spectra in the susceptibility representation of $[C_4C_1C_1C_1N][Tf_2N]$. Black line: room temperature, atmospheric pressure; red line: 190 K, atmospheric pressure; green line: room temperature, 1.1 GPa. The inset shows the data at room condition (black dots), the total curve fit (red line), and the vibrational components of the curve fit (blue lines).

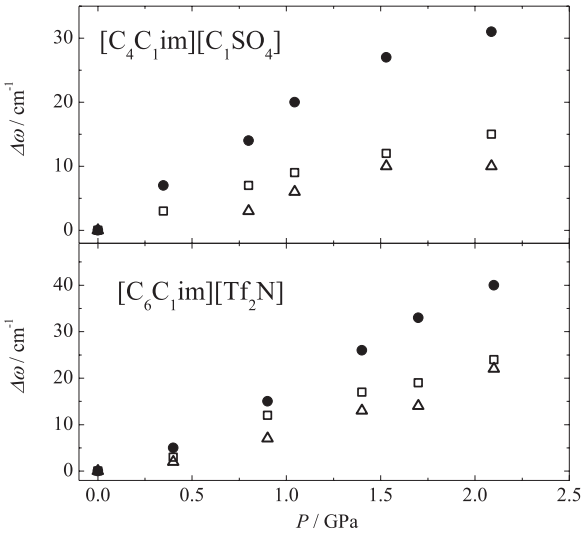

FIG. 7. Pressure induced frequency shifts of the intermolecular vibrations of $[C_4C_1im][C_1SO_4]$ (top panel) and $[C_6C_1im][Tf_2N]$ (bottom panel). The frequencies are given as the difference from the atmospheric pressure value for each of the three components observed at $\sim$20 cm^{-1} (white squares), $\sim$70 cm^{-1} (white triangles), and $\sim$100 cm^{-1} (black circles) at atmospheric pressure.

The comparison of Raman spectra of different imidazolium ionic liquids provided in Figure 8 unravels the characteristics of molecular structure that affect the position of the lowest frequency vibration. We stress that the spectra shown in Fig. 8 are the raw Raman spectra $I(\omega)$ and not the $\chi''(\omega)$ representation as in Figs. 4–6, because the results of Fig. 8 correspond to $T = 150$ K, i.e., the glassy state, for which the QES intensity is low enough that the vibrational components are clearly seen without any data manipulation. Thus, we can compare Raman spectra of glassy phases of $[C_6C_1im][Tf_2N]$ and $[C_4C_1im][Tf_2N]$, for which crystallization is not observed while cooling the liquid, and also $[C_2C_1im][Tf_2N]$, actually with a small amount of $[C_6C_1im][Tf_2N]$ just to hinder its crystallization. It is clear from Fig. 8 that the position of the lowest frequency Raman band is the same for ionic liquids along

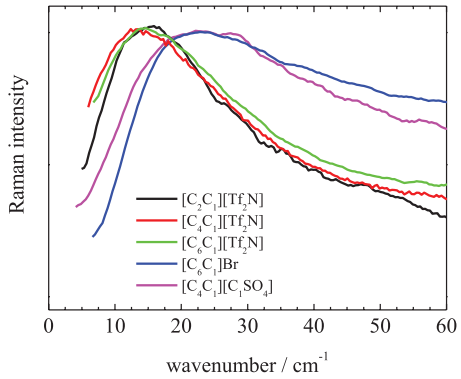

FIG. 8. Raman spectra of glassy phases (150 K, atmospheric pressure) of $[C_2C_1im][Tf_2N]$ (in a binary mixture with molar fraction $x = 0.1$ of $[C_6C_1im][Tf_2N]$, black), $[C_4C_1im][Tf_2N]$ (red), $[C_6C_1im][Tf_2N]$ (green), $[C_6C_1im]Br$ (blue), and $[C_4C_1im][C_1SO_4]$ (magenta).

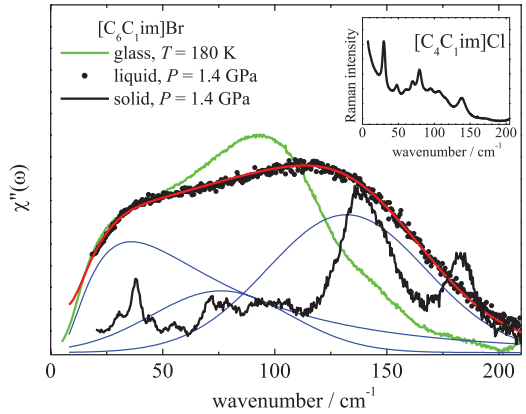

FIG. 9. Raman spectra in the susceptibility representation of $[C_6C_1im]Br$: atmospheric pressure $T = 180$ K (green line); room temperature $P = 1.4$ GPa, after crystallization (black line); room temperature $P = 1.4$ GPa, before crystallization (black circles), with the corresponding curve fit (red line) and individual components of the fit (blue lines). For comparison purposes, the inset shows the Raman spectrum of polycrystalline $[C_4C_1im]Cl$ at ambient conditions.

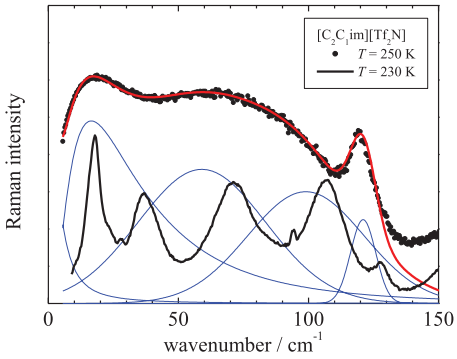

FIG. 10. Raman spectra of $[C_2C_1im][Tf_2N]$: atmospheric pressure $T = 250$ K (black circles, susceptibility representation), with the corresponding curve fit (red line) and individual components of the fit (blue lines); atmospheric pressure $T = 230$ K, after crystallization (black line).

the sequence $[C_2C_1im]^+$, $[C_4C_1im]^+$, and $[C_6C_1im]^+$, while keeping the same $[Tf_2N]^-$ anion. On the other hand, keeping the same $[C_4C_1im]^+$ cation, but replacing the $[Tf_2N]^-$ anion by $[C_1SO_4]^-$, or keeping $[C_6C_1im]^+$ and replacing $[Tf_2N]^-$ by Br^-, the position of this band shifts to a higher frequency. Therefore, the lowest frequency mode of these ionic liquids in a glassy state does not depend on the length of the alkyl chain of the cation. This mode depends instead on the strength of anion–cation interactions as $[Tf_2N]^-$ is replaced by more strongly coordinating anions such as Br^- or $[C_1SO_4]^-$.

Figure 9 shows Raman spectra of a sample of $[C_6C_1Im]Br$ at 1.4 GPa before crystallization (black circles and curve fit by red line) and after crystallization (bold black line). The Raman spectra of $[C_6C_1Im]Br$ before crystallization at 1.4 GPa is similar to the glassy state spectra at 150 K (green line), although it is evident that the vibrational frequency of the librational mode in the low temperature spectrum at $\sim$100 cm^{-1} experiences large shift in the high pressure spectrum. When the sample at high pressure crystallizes, the librational component becomes a relatively sharp band at $\sim$140 cm^{-1} and one also sees another sharp component at $\sim$185 cm^{-1}, which most probably is related to the shoulder at $\sim$150 cm^{-1} in the low temperature Raman spectrum (green line). The Raman spectrum of crystallized $[C_6C_1Im]Br$ at high pressure exhibits sharp bands below 100 cm^{-1} characteristic of a crystalline phase. The blue lines in Fig. 9 are the components used in the curve fit of the amorphous phase spectrum at 1.4 GPa. The two lowest frequency components at $\sim$35 and $\sim$75 cm^{-1} used in the curve fit strongly suggest that they are related to groups of sharp peaks in the crystalline phase spectrum ($30 < \omega < 50$ cm^{-1} and $60 < \omega < 110$ cm^{-1}). For comparison purposes, the inset of Fig. 9 shows the Raman spectrum of $[C_4C_1im]Cl$, which is already a polycrystalline solid at room temperature and atmospheric pressure. Figure 10 shows an analogous comparison for pure $[C_2C_1im][Tf_2N]$, which crystallizes as the temperature of the supercooled liquid decreases below ca. 250 K. The results shown in Fig. 10 suggest that the bands used in the curve fit of the supercooled liquid (blue lines) correspond to broadening of relatively sharp bands that appear in the Raman spectrum of the crystallized sample of $[C_2C_1im][Tf_2N]$ at $T = 230$ K.

IV. DISCUSSION

The finding that the band at $\sim$100 cm^{-1} is absent in Raman spectra of non-aromatic ionic liquids (Fig. 6) indicates that this intermolecular vibration is due to librational motion, i.e., hindered rotation, of the aromatic ring. This assignment has been also proposed by Fujisawa *et al.*,[41] who compared OKE spectra of aromatic and non-aromatic cations ionic liquids based on the $[Tf_2N]^-$ anion. In contrast, Giraud *et al.*[42] assigned all the components of the fit to three librational motions of the cation resulting from three different configurations of anions around the imidazolium ring. However, the two components observed at $\sim$20 cm^{-1} and $\sim$70 cm^{-1} at atmospheric pressure are characteristic features of the Raman spectra regardless of ionic liquids based on aromatic or non-aromatic cations. The distinct pressure induced frequency shift of the librational band (Fig. 7) also suggests that the nature of the band at $\sim$100 cm^{-1} is different from the $\sim$20 and $\sim$70 cm^{-1} components. The microscopic origins of the two low frequency bands could be somehow related, so that both of them undergo a similar frequency shift as they experience the repulsive part of the intermolecular potential with increasing density. Russina *et al.*[43] discussed the OKE spectra of $[C_nC_1im][Tf_2N]$, $n = 2$–9, in the context of dynamics of supercooled liquids, even though obtaining spectra at room temperature. Thus, they assigned the low frequency band at $\sim$20 cm^{-1} to fast β relaxation,[43] which in the terminology of glass-forming liquids is due to restricted translational (rattling) dynamics of a molecule inside the cage formed by the neighboring molecules. In this work, our assignment will also refer to the context of glass-forming liquids, although it is usually considered that low frequency Raman spectra of supercooled liquids exhibit the fast β relaxation as the QES intensity.[19,20,27]

In the phenomenology of Raman and neutron scattering spectra of glass-forming liquids,[19,20,27–29,44,45] the vibrational mode observed at $\sim$20 cm^{-1} in Raman spectra of ionic liquids

in glassy state (Fig. 8) is called the boson peak, which corresponds to intermolecular vibrations in the THz range that are observed as long as the QES intensity decreases at low temperatures. Yamamuro *et al.*[46] also observed the boson peak at ~20 cm^{-1} in the dynamic structure factor $S(k,\omega)$ obtained by neutron scattering spectrum of glassy $[C_4C_1im]Cl$ at $T = 100$ K. In an OKE spectroscopy investigation of 1-ethyl-3-methylimidazolium tosylate, [C2C1im][TSO], Li *et al.*[47] assigned the boson peak to an oscillatory component with a period of ~2.0 ps in the raw time domain data, i.e., a wavenumber of ~17 cm^{-1} in agreement with the Raman spectra of Fig. 8. The boson peak is an excess in the vibrational density of states $g(\omega)$ over the dependence $g_D(\omega) \propto \omega^2$ predicted by the Debye model. Thus, the boson peak is usually considered a peak in the fractional representation $g(\omega)/\omega^2$, although the difference $g(\omega)-g_D(\omega)$ is a more appropriated reconstruction of the excess of the density of states.[40] Unfortunately, there is no experimental data available of sound velocity of ionic liquids at deep supercooled liquid or glassy state to calculate the Debye model prediction $g_D(\omega)$.

It has been shown by neutron or inelastic x-ray scattering (IXS) spectroscopy that the vibrations in the boson peak range have a partial character of transverse acoustic modes of high wavevectors that are hybridized with localized vibrations due to the disorder of the amorphous phase.[35,48–53] In the authors knowledge, collective dynamics of ionic liquids has not yet been investigated by IXS spectroscopy. On the other hand, molecular dynamics (MD) simulations have played a crucial role to unravel the mixed nature of sound-like and localized modes within the range $1 < \omega < 100$ cm^{-1}.[52,54–57] In a MD simulation investigation of a model of $[C_4C_1im]Cl$, Urahata and Ribeiro[58] calculated mass current correlation functions, obtaining spectra of transverse (TA) and longitudinal (LA) acoustic modes exhibiting approximately linear dispersion $\omega(k)$ within the ranges $15 < \omega < 50$ cm^{-1} for TA modes and $30 < \omega < 90$ cm^{-1} for LA modes. It is worth stressing that even in case of sharp spectra of LA and TA modes, the actual eigenvectors of vibrations in this frequency range is a mixture of partial character of sound-like and random phase modes.[35,48,49,56]

A correlation length $\xi = v_s/(2\omega_{bp})$, where ω_{bp} is the boson peak frequency and v_s is the sound velocity of the material, is usually assigned to the boson peak $\xi \sim 10$–30 Å.[28,29,45,59,60] Quitmann and Soltwisch[61] proposed that the first sharp diffraction peak observed at $k_{FSDP} \sim 1.0$ $Å^{-1}$ in the static structure factor $S(k)$ of many different glass forming liquids is a signature of the intermediate range order that provides the underlying structure that sustains the dynamics of the boson peak. In the particular case of ionic liquids, experimental and computer simulation evidences indicate nanoscale heterogeneity due to segregation of the carbon chains of the cations in non-polar domains, whereas the more polar part of the cations and nearby anions result in polar domains.[5,11] Accordingly, the position of a low k peak observed in $S(k)$ of ionic liquids shifts to a lower wavevector as the length of the alkyl chain increases.[11] Therefore, the Raman spectra shown in Fig. 8 indicate that the correlation length ξ assigned to the boson peak is not related to the length scale of non-polar segregation in ionic liquids. The boson peak frequency

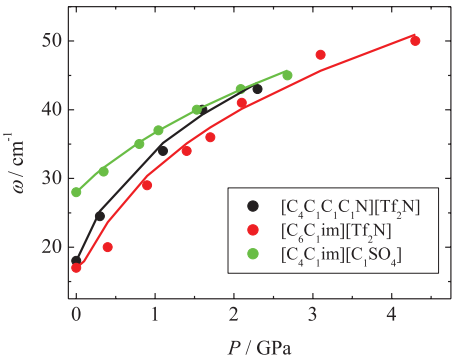

FIG. 11. Pressure dependence of the lowest frequency vibration observed in the susceptibility representation of the Raman spectra of $[C_4C_1C_1C_1N][Tf_2N]$, $[C_6C_1im][Tf_2N]$, and $[C_4C_1im][C_1SO_4]$. The corresponding full lines is the fit by the equation $\omega(P) = \omega_o(1+P/\Lambda)^{1/3}$, with parameters ($\omega$/$cm^{-1}$; Λ/GPa): (18; 0.17), (17; 0.16), and (28; 0.80), respectively.

depends instead on the strength of anion–cation interactions. The first spectral moment $\langle\omega\rangle$ of low frequency OKE spectra of nonaromatic ionic liquids has been related to another criteria of the strength of ionic interactions, namely the surface tension.[10,12] In fact, more stiff polar domains depending on the strength of anion–cation interactions have another experimental consequence: the sound velocity of different ionic liquids does not depend on the length of the alkyl chain if the anion is the same, but it depends instead on changing the anion for a given cation.[62,63]

Focusing on the density of states of quasi-localized vibrations, Gurevich *et al.*[64,65] predicted that the pressure dependence of the boson peak is $\omega(P) = \omega_o(1+P/\Lambda)^{1/3}$, where ω_o is the vibrational frequency at atmospheric pressure and Λ is a parameter related to the compressibility and the random force distribution experienced by quasi-local vibrations. Figure 11 shows that this pressure dependence holds for the lowest frequency vibration in $\chi''(\omega)$ spectra at room temperature for $[C_4C_1C_1C_1N][Tf_2N]$, $[C_6C_1im][Tf_2N]$, and $[C_4C_1im][C_1SO_4]$, with the best fit Λ parameter, respectively, 0.17, 0.16, and 0.80 GPa. The similar Λ parameter for $[C_4C_1C_1C_1N][Tf_2N]$ and $[C_6C_1im][Tf_2N]$, whereas a considerably higher Λ parameter for $[C_4C_1im][C_1SO_4]$, is in line with the proposition of stiffer polar domains for a system with the more strongly coordinating $[C_1SO_4]^-$ anion than the $[Tf_2N]^-$ anion. The $\omega(P)$ dependence shown in Fig. 11 indicates that for relatively high pressure above ca. 2.0 GPa, the data tend to similar values regardless of the molecular structure of the ionic species. In other words, the systems are so heavily packed at high pressures that any difference on ionic structures between these two anions becomes less important and the intermolecular vibrational frequency tends to essentially the same value for these different ionic liquids.

We found a support in favor that the components usually considered in curve fit of Raman spectra of ionic liquids have real physical meaning by considering Raman spectra of systems that undergo at least partial crystallization at low temperatures or high pressures. It is interesting to find correspondence between the intermolecular vibrational motions of ionic liquids in the normal liquid state and excitations of

solid-like domains that might develop in the bulk. The comparisons provided in Figs. 9 and 10 strongly suggest that the components used in the fit of Raman spectra of ionic liquids in amorphous phases have a counterpart in the crystalline phase, although inhomogeneously broadened by structural disorder of the amorphous phases. Once the boson peak has been assigned to mixing between localized modes and high frequency transverse acoustic plane waves, we propose that the other component observed at $\sim$70 cm^{-1} has a mixed character of local modes with longitudinal acoustic modes. Assigning the intermolecular vibrations at $\sim$20 and $\sim$70 cm^{-1} to partial character of acoustic excitations is consistent with the fact that both of them are found independently of specific molecular structure either in aromatic or non-aromatic ionic liquids (Figs. 5 and 6), the similar shifts of vibrational frequencies with increasing pressure (Fig. 7), the dependence of the peak position with the strength of anion–cation interactions (Fig. 8), and the pressure dependence according to the model of Gurevich *et al.*[64,65] (Fig. 11). However, it is worth stressing that there is not a sharp distinction between transverse and acoustic nature for high-(k,ω) excitations because of strong mixing between them and localized vibrations.[35,48–50,56,57,66]

The relationship between low frequency Raman spectra of amorphous phases and the spectra of partially crystallized samples (Figs. 9 and 10) has been also observed in other glass formers, e.g., butanol,[67] triphenylphosphite,[68,69] and salol.[70] The situation has been characterized as microcrystallites immersed in an amorphous phase and called glacial state. It is worth noting that these solid domains do not necessarily have the same structure of the thermodynamically stable crystalline phase. In fact, the common finding is that the broad bands observed in low frequency Raman spectra of glasses barely indicate a direct correspondence with the complex many sharp peaks due to phonons observed in Raman spectra of crystals.[71–74] For comparison purposes, the inset of Fig. 9 shows the rather different Raman spectrum of [C_4C_1im]Cl, which is a solid at room temperature and pressure. In contrast, Raman spectra of some partially crystallized ionic liquids are analogous to spectra observed for glacial state of molecular glass formers[67–70] and also direct visualization of the resulting opaque suggests there is a mixture of crystallites and amorphous phase. Such a physical picture of the glacial state was supported by Kivelson and Tarjus[75] according to the model of local frustrated domains, as nuclei growing could be frustrated in such a spatial dimension that is in the very borderline between a crystalline phase or solid-like amorphous domain. Although the model of Tanaka[59] is also based on the idea of frustration, his two-order parameter model considers an energetic frustration of local bonds against density optimization that would lead to crystallization, whereas Kivelson and Tarjus[75] emphasizes a local structure in the liquid that is geometrically frustrated as it does not fit the whole space in a crystalline array. Nevertheless, the physical picture is that metastable solid-like domains that could exist in the supercooled liquid, consistent with the same idea proposed on the basis of the complex pattern of the DSC scans of ionic liquids.[36,38,39] All of these findings suggest mesoscopic ordering in supercooled liquids[75–79] and in the particular case of ionic liquids that order might be beyond the nanoscale heterogeneity of polar/non-polar domains segregation.

V. CONCLUSIONS

The effect of pressure on low frequency Raman spectra of ionic liquids is much more strong than the effect of temperature along the supercooled liquid range. Investigating the dependence of vibrational frequencies with pressure provides further insights on the microscopic origin of intermolecular vibrational dynamics of ionic liquids. The vibrational component assigned to librational motion of aromatic cations observed at $\sim$100 cm^{-1} at atmospheric pressure exhibits larger pressure induced shift than the other two components observed at lower frequencies. The so-called boson peak is observed in Raman spectra of ionic liquids in deeply supercooled liquid and glassy states. Although non-polar/polar heterogeneity of ionic liquids should imply the coexistence of relatively softer and stiffer domains in ionic liquids, the actual position of the boson peak is not dependent on the dimension of non-polar segregation as the alkyl chain of cations increases. The boson peak frequency is dependent instead on changing the anion for a given cation. The components observed at $\sim$20 and $\sim$70 cm^{-1} at room conditions exhibit similar shift with increasing pressure and these two spectral features are not dependent on details of ionic structures as they are observed in Raman spectra of both aromatic and non-aromatic ionic liquids. The pressure-induced shift of the lowest frequency component in the $\chi''(\omega)$ spectra at room temperature follows the $P^{1/3}$ dependence predicted for the boson peak. There is a correspondence of the broad vibrational components in low frequency Raman spectra of ionic liquids and relatively sharp peaks characteristic of Raman spectra of a solid phase that develops as an ionic liquid experiences partial crystallization at low temperature or high pressure. We propose there is mixing between localized motions and plane wave excitations of high wavevectors in the low frequency vibrations of ionic liquids.

ACKNOWLEDGMENTS

The authors would like to thank Dr. Fernando A. Sigoli and Dr. Ítalo O. Mazali for the availability of the Raman spectrometer with a coupled microscope at the Laboratório Multiusuário de Espectroscopia Óptica Avançada at UNICAMP. The authors are indebted to FAPESP and CNPq for financial support.

[1] L. Larini, A. Ottochian, C. De Michele, and D. Leporini, Nat. Phys. **4**, 42 (2008).
[2] J. C. Dyre, Rev. Mod. Phys. **78**, 953 (2006).
[3] G. Adam and J. H. Gibbs, J. Chem. Phys. **43**, 139 (1965).
[4] D. Turnbull and M. H. Cohen, J. Chem. Phys. **52**, 3038 (1970).
[5] E. W. Castner and J. F. Wishart, J. Chem. Phys. **132**, 120901 (2010).
[6] A. V. Blokhin, Y. U. Paulechka, A. A. Strechan, and G. J. Kabo, J. Phys. Chem. B **112**, 4357 (2008).
[7] A. V. Blokhin, Y. U. Paulechka, and G. J. Kabo, J. Chem. Eng. Data **51**, 1377 (2006).
[8] A. Fernandez, J. S. Torrecilla, J. Garcia, and F. Rodriguez, J. Chem. Eng. Data **52**, 1979 (2007).

[9]C. P. Fredlake, J. M. Crosthwaite, D. G. Hert, S. N. V. K. Aki, and J. F. Brennecke, J. Chem. Eng. Data **49**, 954 (2004).
[10]H. Fukazawa, T. Ishida, and H. Shirota, J. Phys. Chem. B **115**, 4621 (2011).
[11]O. Russina, A. Triolo, L. Gontrani, and R. Caminiti, J. Phys. Chem. Lett. **3**, 27 (2012).
[12]H. Shirota, ChemPhysChem **13**, 1638 (2012).
[13]D. A. Turton, J. Hunger, A. Stoppa, G. Hefter, A. Thoman, M. Walther, R. Buchner, and K. Wynne, J. Am. Chem. Soc. **131**, 11140 (2009).
[14]D. A. Turton, T. Sonnleitner, A. Ortner, M. Walther, G. Hefter, K. R. Seddon, S. Stana, N. V. Plechkova, R. Buchner, and K. Wynne, Faraday Discuss. **154**, 145 (2012).
[15]A. Triolo, O. Russina, H. J. Bleif, and E. Di Cola, J. Phys. Chem. B **111**, 4641 (2007).
[16]A. Wulf, K. Fumino, R. Ludwig, and P. F. Taday, ChemPhysChem **11**, 349 (2010).
[17]K. Fumino, K. Wittler, and R. Ludwig, J. Phys. Chem. B **116**, 9507 (2012).
[18]A. Chakraborty, T. Inagaki, M. Banno, T. Mochida, and K. Tominaga, J. Phys. Chem. A **115**, 1313 (2011).
[19]M. C. C. Ribeiro, J. Chem. Phys. **133**, 024503 (2010).
[20]M. C. C. Ribeiro, J. Chem. Phys. **134**, 244507 (2011).
[21]T. Takekiyo, Y. Imai, N. Hatano, H. Abe, and Y. Yoshimura, Chem. Phys. Lett. **511**, 241 (2011).
[22]H. C. Chang, J. C. Jiang, J. C. Su, C. Y. Chang, and S. H. Lin, J. Phys. Chem. A **111**, 9201 (2007).
[23]L. Su, X. Zhu, Z. Wang, X. R. Cheng, Y. Q. Wang, C. S. Yuan, Z. P. Chen, C. L. Ma, F. F. Li, Q. Zhou, and Q. L. Cui, J. Phys. Chem. B **116**, 2216 (2012).
[24]O. Russina, B. Fazio, C. Schmidt, and A. Triolo, Phys. Chem. Chem. Phys. **13**, 12067 (2011).
[25]L. Su, M. Li, X. Zhu, Z. Wang, Z. P. Chen, F. F. Li, Q. Zhou, and S. M. Hong, J. Phys. Chem. B **114**, 5061 (2010).
[26]H. C. Chang, J. C. Jiang, W. C. Tsai, G. C. Chen, and S. H. Lin, J. Phys. Chem. B **110**, 3302 (2006).
[27]L. Hong, B. Begen, A. Kisliuk, V. N. Novikov, and A. P. Sokolov, Phys. Rev. B **81**, 104207 (2010).
[28]L. Hong, P. D. Gujrati, V. N. Novikov, and A. P. Sokolov, J. Chem. Phys. **131**, 194511 (2009).
[29]L. Hong, V. N. Novikov, and A. P. Sokolov, Phys. Rev. E **83**, 061508 (2011).
[30]M. Krummen, P. Wasserscheid, and J. Gmehling, J. Chem. Eng. Data **47**, 1411 (2002).
[31]R. G. de Azevedo, J. M. S. S. Esperanca, J. Szydlowski, Z. P. Visak, P. F. Pires, H. J. R. Guedes, and L. P. N. Rebelo, J. Chem. Thermodyn. **37**, 888 (2005).
[32]W. A. Bassett, High Press. Res. **29**, 163 (2009).
[33]H. Tokuda, K. Hayamizu, K. Ishii, M. A. B. H. Susan, and M. Watanabe, J. Phys. Chem. B **109**, 6103 (2005).
[34]G. Annat, M. Forsyth, and D. R. MacFarlane, J. Phys. Chem. B **116**, 8251 (2012).
[35]P. M. Derlet, R. Maass, and J. F. Loffler, Eur. Phys. J. B **85**, 148 (2012).
[36]M. Imanari, K. Fujii, T. Endo, H. Seki, K. Tozaki, and K. Nishikawa, J. Phys. Chem. B **116**, 3991 (2012).
[37]L. F. O. Faria, J. R. Matos, and M. C. C. Ribeiro, J. Phys. Chem. B **116**, 9238 (2012).
[38]K. Nishikawa, S. Wang, and K. I. Tozaki, Chem. Phys. Lett. **458**, 88 (2008).
[39]K. Nishikawa and K. Tozaki, Chem. Phys. Lett. **463**, 369 (2008).
[40]S. N. Yannopoulos, K. S. Andrikopoulos, and G. Ruocco, J. Non-Cryst. Solids **352**, 4541 (2006).
[41]T. Fujisawa, K. Nishikawa, and H. Shirota, J. Chem. Phys. **131**, 244519 (2009).
[42]G. Giraud, C. M. Gordon, I. R. Dunkin, and K. Wynne, J. Chem. Phys. **119**, 464 (2003).
[43]O. Russina, A. Triolo, L. Gontrani, R. Caminiti, D. Xiao, L. G. Hines, R. A. Bartsch, E. L. Quitevis, N. Pleckhova, and K. R. Seddon, J. Phys.: Condes. Matter **21**, 424121 (2009).
[44]S. N. Yannopoulos and G. N. Papatheodorou, Phys. Rev. B **62**, 3728 (2000).
[45]A. P. Sokolov, A. Kisliuk, D. Quitmann, A. Kudlik, and E. Rossler, J. Non-Cryst. Solids **172**, 138 (1994).
[46]O. Yamamuro, Y. Inamura, S. Hayashi, and H. Hamaguchi, AIP Conf. Proc. **832**, 73 (2006).
[47]J. Li, I. Wang, K. Fruchey, and M. D. Fayer, J. Phys. Chem. A **110**, 10384 (2006).
[48]G. Monaco and V. M. Giordano, Proc. Natl. Acad. Sci. U.S.A. **106**, 3659 (2009).
[49]H. Shintani and H. Tanaka, Nat. Mater. **7**, 870 (2008).
[50]G. Ruocco and F. Sette, J. Phys.:Condes. Matter **13**, 9141 (2001).
[51]C. Cabrillo, F. J. Bermejo, A. Maira-Vidal, R. Fernandez-Perea, S. M. Bennington, and D. Martin, J. Phys.:Condes. Matter **16**, S309 (2004).
[52]U. Balucani and M. Zoppi, *Dynamics of the Liquid State* (Oxford University Press, 1994).
[53]G. Ruocco and F. Sette, J. Phys.:Condes. Matter **11**, R259 (1999).
[54]M. C. C. Ribeiro, J. Chem. Phys. **114**, 6714 (2001).
[55]M. C. C. Ribeiro, J. Chem. Phys. **137**, 104510 (2012).
[56]M. C. C. Ribeiro, M. Wilson, and P. A. Madden, J. Chem. Phys. **108**, 9027 (1998).
[57]M. C. C. Ribeiro, M. Wilson, and P. A. Madden, J. Chem. Phys. **110**, 4803 (1999).
[58]S. M. Urahata and M. C. C. Ribeiro, J. Chem. Phys. **124**, 074513 (2006).
[59]H. Tanaka, J. Non-Cryst. Solids **351**, 3396 (2005).
[60]A. P. Sokolov, A. Kisliuk, M. Soltwisch, and D. Quitmann, Phys. Rev. Lett. **69**, 1540 (1992).
[61]D. Quitmann and M. Soltwisch, Philos. Mag. B **77**, 287 (1998).
[62]M. Fukuda, M. Terazima, and Y. Kimura, J. Chem. Phys. **128**, 114508 (2008).
[63]C. Frez, G. J. Diebold, C. D. Tran, and S. Yu, J. Chem. Eng. Data **51**, 1250 (2006).
[64]V. L. Gurevich, D. A. Parshin, and H. R. Schober, Phys. Rev. B **67**, 094203 (2003).
[65]V. L. Gurevich, D. A. Parshin, and H. R. Schober, Phys. Rev. B **71**, 014209 (2005).
[66]E. Duval, A. Mermet, and L. Saviot, Phys. Rev. B **75**, 024201 (2007).
[67]A. Wypych, Y. Guinet, and A. Hedoux, Phys. Rev. B **76**, 144202 (2007).
[68]A. Hedoux, Y. Guinet, M. Descamps, O. Hernandez, P. Derollez, A. J. Dianoux, M. Foulon, and J. Lefebvre, J. Non-Cryst. Solids **307**, 637 (2002).
[69]Y. Guinet, T. Denicourt, A. Hedoux, and M. Descamps, J. Mol. Struct. **651**, 507 (2003).
[70]J. Baran, N. A. Davydova, and M. Drozd, J. Phys.: Condes. Matter **22**, 155108 (2010).
[71]A. Criado, F. J. Bermejo, A. Deandres, and J. L. Martinez, Mol. Phys. **82**, 787 (1994).
[72]H. M. Flores-Ruiz and G. G. Naumis, Phys. Rev. B **82**, 214201 (2010).
[73]D. Quitmann and M. Soltwisch, J. Non-Cryst. Solids **235**, 237 (1998).
[74]F. J. Bermejo, A. Criado, A. deAndres, E. Enciso, and H. Schober, Phys. Rev. B **53**, 5259 (1996).
[75]D. Kivelson and G. Tarjus, J. Non-Cryst. Solids **307**, 630 (2002).
[76]S. A. Kivelson, X. L. Zhao, D. Kivelson, T. M. Fischer, and C. M. Knobler, J. Chem. Phys. **101**, 2391 (1994).
[77]H. Tanaka, J. Chem. Phys. **111**, 3163 (1999).
[78]P. G. de Gennes, C. R. Phys. **3**, 1263 (2002).
[79]H. Shintani and H. Tanaka, Nat. Phys. **2**, 200 (2006).